Effects of Mixing Water Salinity on the Properties of Concrete

Tanaz Dhondy [1, 2], Y. Xiang [2], T. Yu [2], and J. G. Teng [2*]

[1] School of Civil, Mining & Environmental Engineering, University of Wollongong, Wollongong, NSW 2522, Australia

[2] Department of Civil and Environmental Engineering, The Hong Kong Polytechnic University, Hong Kong, China

ABSTRACT

The use of seawater and sea-sand in producing concrete has attracted increasing research attention in recent years to address the shortage of river sand and in certain applications the shortage of freshwater. In particular, reinforced concrete structures made of seawater sea-sand concrete (SSC) and corrosion-resistant fiber-reinforced polymer (FRP) are particularly attractive for the development of coastal and marine infrastructure (e.g., on remote islands) as durable structures can be created using locally available materials. Existing studies on SSC or seawater concrete have been largely limited to the use of mixing water with a salinity level close to the world-average ocean salinity. Against this background, the present paper reports the first ever systematic study on the effect of salinity of mixing water on the properties of concrete. The present study covered a wide range of salinity levels from 16.5 g/L to 82.5 g/L, and examined a wide range of short-term concrete properties including the heat of hydration, shrinkage, compressive strength and modulus of elasticity. The test results show that the salinity of mixing water has a considerable effect on the rate of hydration heat and shrinkage at early ages, as well as the cumulative release of hydration heat. It is also shown that the water salinity has a slight negative effect on the compressive strength and modulus of elasticity of concrete at ages older than 14 days.

Keywords: Seawater; Concrete; Salinity; Concrete properties; Shrinkage; Compressive strength.

* Corresponding Author:
Department of Civil and Environmental Engineering, The Hong Kong Polytechnic University, Hong Kong, China. Email: cejgteng@polyu.edu.hk.

1. INTRODUCTION

Concrete is the second most consumed material by the human society on the planet after water (Gagg 2014). The increasing demand for concrete has imposed a significant strain on natural resources, including freshwater and river sand. Furthermore, concrete is normally used together with steel reinforcement which is prone to corrosion. To address these problems, the corresponding author of the present study proposed a new type of concrete structures involving the use of concrete made with seawater and sea-sand in combination with fiber-reinforced polymer (FRP) reinforcement which does not corrode (Teng et al. 2011; Teng 2014). The new type of structures is particularly attractive for use in infrastructure development along coastlines and on islands where seawater and sea-sand are readily available but river sand and freshwater are not easily accessible.

As a major constituent material, the mixing water affects the workability, strength development and durability of concrete. Seawater consists of a range of chemicals which can affect the fresh and hardened properties of concrete (Xiao et al. 2017). Extensive experimental studies (Taylor 1978; Ghorab et al. 1989 and 1990; Kaushik and Islam 1995; Nishida et al. 2013; Dhondy et al. 2019; Li et al. 2018; Younis et al. 2018; Teng et al. 2019; Li et al. 2020; Huang et al. 2020) have been conducted on seawater concrete of various strengths, ranging from normal strength concrete (e.g. Kaushik and Islam 1995; Younis et al. 2018; Li et al. 2020) to ultrahigh strength concrete with a compressive strength of over 180 MPa (Teng et al. 2019). Many of these studies (e.g. Ghorab et al 1990; Teng et al. 2019) were focused on the mechanical properties, in particular the compressive strength, of seawater concrete. It has been shown that the use of seawater as mixing water may lead to an increase in the early-age strength of concrete, but the long-term strength of seawater concrete is similar to or lower than that of freshwater concrete with the same mix proportions (Nishida et al. 2013; Younis et al. 2018).

The development of concrete strength is known to be associated with the hydration process. More recently, Younis et al. (2018) found that the rate of hydration heat of seawater sea-sand concrete was higher than that of concrete made with freshwater and river sand at early ages, which may partially explain the relatively high early strength of the former. In the same study, Younis et al. (2018) observed that the use of seawater may lead to increased drying shrinkage of concrete as a result of the presence of chloride ions.

While the existing studies have identified some important differences between seawater concrete and freshwater concrete, most of them were limited to the use of water with a salinity [defined herein as the total amount of salts dissolved in a solution (Makhlouf 2014; Gieskes 2007; Taylor 1978)] level equal or close to the world-average ocean salinity (i.e. 35 g/L) (Hay et al. 2001; NOAA 2018). Therefore, these studies did not allow the effect of varying the salinity level on the properties of concrete to be clearly revealed. For the same reason, their results are not applicable to concrete made with saltwater obtained from locations where the salinity level is significantly different from the world-average value. For example, the Dead Sea in Jordan has a salinity of 34%, while the Great Salt Lake in the USA has a salinity varying between 5%-27% (NASA 2014). The existing studies on saltwater concrete with varying salinities have been quite limited (Kaushik and Islam 1995; Teng et al. 2019). Kaushik and Islam (1995) produced concrete with saltwater of salinities of up to 10 times the world-average ocean salinity, but their studies were focused only on the compressive strength of concrete. Teng et al. (2019) reported a recent study by the authors' group aimed at development of ultrahigh performance seawater sea-sand concrete. Therefore, for a better understanding of the effect of mixing water salinity and the behavior of concrete produced with mixing water of high salinity, a study on the effect of salinity over a wide range of salinity levels is highly valuable.

Against this background, the paper presents the first ever systematic experimental study on the effect of mixing water salinity on the properties of normal strength concrete. The experimental study covered a wide range of salinity levels and examined a wide range of short-term concrete properties including the heat of hydration, shrinkage, compressive strength, and modulus of elasticity.

2. EXPERIMENTAL PROGRAMME

2.1 Mix Design

In the present study, six groups of specimens were prepared and tested, as detailed in Table 1. Group 1 was mixed with tap water and served as the control group. Groups 2 to 5 were mixed with saltwater, which was made with tap water and dissolved commercial sea salt (Red Sea 2017) of five different doses, respectively. The doses of sea salt in the mixing water of Groups 2 to 5 ranged from 18 g/L to 90 g/L with an interval of 18 g/L, so as to simulate saltwater with salinity levels of 50% to 250% of the world-average ocean salinity.

2.2 Raw Materials

A Type I ordinary Portland cement conforming to BS EN 197-1 (2000) was used as the only binding material of the concrete mix. The chemical and phase compositions of the cement were analysed using X-ray fluorescence (XRF) spectroscopy (AXS GmbH, Bruker), and are given in Table 2.

[Insert Table 1]

[Insert Table 2]

Natural river sand with the maximum particle size being 5 mm and crushed granite with the maximum particle size being 10 mm were used as the fine and the coarse aggregates, respectively. A polycarboxylate-based superplasticizer (ADVA® 189) was added to ensure the workability of concrete. The superplasticizer used in the concrete had a specific gravity of 1.06 and a solid content of 35% by mass.

The chemical compositions of the water samples from Groups 1 (i.e. tap water) and 3 (i.e. with sea salt at 36 g/L) were analysed by Ion chromatography (IC) tests. Table 3 compares the test results with those of natural seawater sampled from two locations along the coast of Hong Kong and the world-average composition. It is seen that the saltwater produced with a sea salt dose of 36 g/L (i.e. Group 3) achieved a salinity of about 33 g/L, due to the existence of organic chemicals and water in the sea salt which did not contribute to the salinity level. This salinity level is slightly lower than the world-average value (i.e. 35 g/L) but close to those of the two local seawater samples. To avoid any confusion, the measured salinity is used hereafter in the paper. That is, for Groups 2-6, the salinities were 16.5 g/L, 33.0 g/L, 49.5 g/L, 66.0 g/L and 82.5 g/L, respectively.

[Insert Table 3]

2.3 Methodology

2.2.1 Mixing, Casting and Curing of Concrete

The concrete was mixed in two stages. The dry constituents (i.e. cement, fine and coarse aggregates) were first mixed for 5 minutes. The water and the superplasticiser were then added before mixing for another 8 minutes until the concrete reached an acceptable level of consistency. Slump tests were conducted on each group after mixing in accordance with ASTM C143/143M (ASTM 2015).

The freshly mixed concrete was cast and compacted on a vibration table for 1 minute. After casting, all moulds were covered with plastic sheets in ambient conditions for 24 hours. The specimens were then demoulded and placed in a curing chamber which maintained the curing conditions at a temperature of 23±2 °C and a humidity of 50%.

2.2.2 Isothermal Calorimetry

Isothermal calorimetry tests were performed on the cement paste specimens of all groups following ASTM C1679 (ASTM 2017). For each group, cement paste of 180±0.1 g was poured into a plastic ampule and then placed in an isothermal calorimeter (I-Cal 4000, Calmetrix) which was preconditioned to a temperature of 23 ± 0.05 °C. The rate of hydration heat and cumulative heat release were measured for 72 hours and normalized by the mass of cement.

2.2.3 Shrinkage

The shrinkage of Groups 1, 3 and 5 was determined with the following procedure (Younis et al. 2018; Lu et al. 2017): (1) the concrete was cast into rectangular prisms with dimensions of 75 mm × 75 mm × 280 mm; (2) the initial dimensions and masses of all prisms were measured 24 hours after casting; and (3) subsequently, the length and mass changes of each specimen were measured with an interval of 1 day up to 14 days, and then at the ages of 21, 28, 60 and 90 days.

The above procedure was adopted so that the measurements represent the development of shrinkage of concrete after demolding. As the hydration process of concrete continues after 24 hours, the measured shrinkage includes both autogenous shrinkage and drying shrinkage. It should be noted that this procedure is different from that specified in ASTM C157 (ASTM 2017b), in which the length change is measured after the concrete is immersed in limewater until an age of 28 days. Due to the salinity of mixing water in the present study, the procedure in ASTM C157 (ASTM 2017b) may not be suitable here as the immersion of specimens in limewater may cause loss of its salinity.

2.2.4 Compressive Behaviour and Modulus of Elasticity

The concrete was cast into cylinders of a diameter of 100 mm and a height of 200 mm, which were tested at the ages of 1, 7, 14, 28 and 90 days in accordance with ASTM C469/C469M (ASTM 2014). For each group at each age, three specimens were tested. The tests were completed using a M500-50 computer controlled universal materials testing machine (Testometric, UK) with a stress control rate of 0.6 MPa/s. Two Linear Variable Displacement Transducers (LVDTs) were mounted at 180° apart from each other on each cylinder to measure the axial deformation of the 120 mm mid-height region, which was then used to calculate the modulus of elasticity of each specimen in accordance with ASTM C469/C469M (ASTM 2014).

3. RESULTS AND DISCUSSIONS

3.1 Heat Evolution

The effects of varying salinity on the rate of hydration heat and cumulative heat release of the cement paste are shown in Figure 1. By comparing the curves of Group 1 and those of Groups 2 to 6, it is evident that the existence of salt in the mixing water had a significant effect on both the hydration process (Figure 1a) and the cumulative heat release (Figure 1b). The rate of hydration heat at the second peak was 2.51 mW/g at 13.5 hours for Group 1 mixed with tap water. By contrast, for Group 2 mixed with saltwater having a salinity of 16.5 g/L, the second peak occurred much earlier (i.e. at 9.90 hours), with a significantly higher rate of hydration heat (i.e. 3.36 mW/g). Despite the significant differences between Group 1 and Group 2, it is interesting to note that a further increase in salinity from 16.5 g/L (Group 2) to 82.5 g/L (Group 6) only had a small effect on the hydration process (Figure 1a). Similar observations can also be made from Figure 1b: the cumulative heat release increases with the salinity of mixing water, but at a decreasing rate.

The above observations are generally consistent with the results from exiting studies (Ghorab et al. 1989; Shi et al. 2015; Li et al. 2018; Younis et al. 2018), which suggested that the presence of salt in the mixing water accelerated the hydration process and increased the heat release. These observed effects of salt may be due to: (1) the reaction of sodium chloride (NaCl) from saltwater with the calcium hydroxide ($Ca(OH)_2$) in the concrete pore solution to form calcium chloride ($CaCl_2$), which accelerates the early-age hydration process (Peterson and Juenger 2006); and/or (2) the diffusion of small Cl^- ions into the passivating layer of the metastable calcium-silicate-hydrate (C-S-H), which increases the internal pressure of the metastable C-S-H and promotes the rupture of the passivating layer, leading to an accelerated hydration process by facilitating contact between the cement clinker (C_3S) and water (Singh and Ojha 1981; Cheung et al. 2011).

3.2 Shrinkage

The development of shrinkage with time is shown in Figure 2 for Groups 1, 3 and 5. The overall trend of the three curves in Figure 2 is similar: the shrinkage increases with time at a decreasing rate for all groups. By comparing the curves of the three groups, it is evident that before the age of 21 days, the rate of shrinkage development increases significantly with the salinity of the mixing water. This effect, however, becomes less pronounced after 21 days when the shrinkage develops at a relatively slow rate for all groups (Figure 2). For example, the shrinkage strains at the age of

21 days were 316 με, 582 με and 834 με, respectively, for Groups 1, 3 and 5, while the strains at the age of 90 days for the three groups were 428 με, 762 με and 1038 με, respectively.

[Insert Figure 2]

The effect of salinity on the shrinkage strain at the ages of 7, 21 and 90 days is shown in Figure 3. It is evident that the shrinkage strain increases almost linearly with the salinity at all the ages. To further examine the correlations, the best-fit line and equation for each of the three ages are also shown in Figure 3. It is not surprising to see that the downward slope of the line increases with time, as the difference in the shrinkage strain among the three groups keeps increasing, suggesting that the salinity of mixing water has a sustained effect on the shrinkage of concrete.

[Insert Figure 3]

Autogenous shrinkage and drying shrinkage are two main forms of concrete shrinkage, with the former being related to the consumption of water in the hydration process (Hua et al. 1995) and the latter being related to the evaporation of free water (Hansen 1987; Bakhshi et al. 2012). Both forms of shrinkage are generally accepted as a result of capillary tension (Hansen 1987; Hua et al. 1995; Lura et al. 2003; Li and Li 2014). The term "capillary tension" refers to the hydrostatic tension exerted by the water meniscus in capillary pores of concrete, which increases with the loss of water and the reduction of pore size, and contributes to the overall contraction of the concrete.

In accordance with the mechanism, capillary tension is highly related to the moisture and pore size distribution of concrete (Hansen 1987). Therefore, the observed effect of salinity, as discussed above, is believed to be due to the combined effect of: (1) accelerated hydration (see Figure 1) which leads to increased consumption of water and thus increased autogenous shrinkage (Li et al. 2018; Khatibmasjedi et al. 2019); and (2) the refined pore structure of concrete caused by the presence of NaCl and $CaCl_2$, leading to an increased number of small pores in the size range of 3 nm to 20 nm in the concrete (Suryavanshi et al. 1995; Park et al. 2011; Younis et al. 2019). The number of such small pores was observed to increase with the salinity level (Vanhanen et al. 2008), which accounts for the increase of capillary action and drying shrinkage.

[Insert Figure 4]

The effect of salinity on shrinkage may also be partially due to the increased heat release associated with an increase in salinity (Figure 1). The increased heat release is expected to have led to an increase in the speed of water evaporation from the concrete. This is evidenced by the change of mass with time of the three groups (Figure 4), considering that the mass loss of concrete mainly results from the evaporation of internal water (Bakhshi et al. 2012).

3.3 Compressive Strength

The development of compressive strength with time is shown in Figures 5a and 5b for all groups, while the detailed test results are summarized in Table 4. In Figure 5b, the compressive strengths are normalized by the respective 1-day strength of each group for ease of comparison. Figure 5 shows that for all groups, the compressive strength develops significantly within the first 7 days.

After the first 7 days, the compressive strength of Group 1 with tap water still increases considerably, but those of other groups with saltwater do not change so much except for that of Group 6. The strength development of Group 6 follows a similar trend to that of Group 1, but the reason is not clear.

Figure 6 provides further comparisons for the compressive strengths of different groups at various ages. It is evident that the 1-day strengths of Groups 2 and 3 are considerably higher than that of Group 1, suggesting that the use of saltwater with a salinity of up to 33 g/L leads to a higher early strength of concrete. A further increase in salinity, however, is shown to decrease the 1-day strength of concrete (Figure 6a). After 14 days, the strengths of Groups 2-6 are consistently lower than that of Group 1, suggesting that the long-term compressive strength of concrete may be negatively affected by the salinity of mixing water. Furthermore, the strengths of Groups 2 and 3 with lower salinities (16.5-33.0 g/L) after 14 days appear to be considerably higher than the corresponding strengths of Groups 4-6 with higher salinities (49.5-82.5 g/L), while the strengths of Groups 4-6 are similar at all ages.

[Insert Figure 5, Figure 6 and Table 4]

The relatively high early-age compressive strength of concrete mixed with saltwater has been reported by many existing studies (e.g. Kaushik and Islam 1995; Younis et al. 2018; Teng et al. 2019; Li et al. 2020). This is generally believed to be due to the existence of chloride ions, which promotes the the formation of a chloro-AFm phase (i.e. the Friedel's salt) and a chloro-sulphate AFm phase (i.e. Kuzel's salt) (Younis et al. 2018; De Weerdt et al. 2014), and leads to densification of the microstructure of concrete. The test results of the present study indicated that this effect is the most pronounced when the salinity of mixing water is around 33 g/L. The existence of an optimum salinity for the early-age compressive strength has also been reported by Teng et al. (2019) for ultrahigh strength seawater sea-sand concrete. In Teng et al.'s (2019) study, the optimum salinity was found to be approximately 18 g/L for concrete with a water-to-cement ratio (i.e. 0.18) much lower than that in the present study (i.e. 0.6). It may therefore be concluded that the effect of salinity of mixing water is also considerably dependent on the water-to-cement ratio of the concrete mix.

The relatively low long-term compressive strength of saltwater concrete (i.e. Groups 2-6), compared with Group 1, is believed to be due to: (1) the existence of $MgSO_4$ in the seawater which may react with the calcium hydroxide [$Ca(OH)_2$] in the pore solution of concrete, forming expansive products (Uddin et al. 2004; Shayan 2010; De Weerdt et al. 2014); and/or (2) the decomposition of Friedel's salt and Kuzel's salt with time due to carbonation (Suryavanshi and Swamy 1996).

3.4 Modulus of Elasticity

The effect of salinity of mixing water on the modulus of elasticity of concrete at various ages is illustrated in Figure 7. It has been well established that the modulus of elasticity is related to the compressive strength of concrete (Pauw 1960), so it is not surprising to see that the effect of salinity seen in Figure 7 is generally similar to that seen in Figure 6 for the compressive strength. The use of saltwater leads to a decrease in the modulus of elasticity of concrete, and this negative effect appears to increase initially with the salinity level, as evident from the results of Groups 1 to 3. For Groups 4-6 with relatively high salinities (49.5-82.5 g/L), while their moduli of elasticity at all ages are lower than those of Groups 1-3, there is little difference among themselves (i.e. Groups 4-6), suggesting that there may be a limit of the negative effect of salinity.

[Insert Figure 7]

To reveal the relationship between the modulus of elasticity and the compressive strength of saltwater concrete, the test results are shown in Figure 8 against the predictions of the following equations based on the provisions of CEB-FIP (2010) and ACI 209R-92 (2008):

CEB-FIP (2010):

$$E_{\mathrm{c}}(t) = \sqrt{\beta_{\mathrm{cc}}(t)} E_{\mathrm{c0}} \alpha_{\mathrm{E}} \left(\frac{f_c'(t)}{10\beta_{\mathrm{cc}}(t)} \right)^{1/3} \tag{1}$$

$$\beta_{\mathrm{cc}}(t) = exp\left\{ s \left[1 - \left(\frac{28}{t} \right)^{0.5} \right] \right\} \tag{2}$$

ACI 209R-92 (2008):

$$E_{\mathrm{c}}(t) = 0.043 w^{1.5} \sqrt{f_c'(t)} \tag{3}$$

$$f_c'(t) = \frac{t}{\alpha + \beta t} f_c' \tag{4}$$

where $E_{\mathrm{c}}(t)$ is the modulus of elasticity at an age t in days and has a unit of MPa; E_{c0} is equal to 21.5×10^3 MPa; f_c'(t) is the compressive strength of concrete at age t in days and has a unit of MPa; α_{E} is a coefficient accounting for the type of coarse aggregate, and is equal to 1.0 for the aggregate used in the present study (i.e. crushed granite); and s is a coefficient accounting for the cement type and is equal to 0.20 for the cement used in the present study (i.e. 52.5N); α and β are constants determined by the cement type and curing regime of concrete, taking the values of 4 and 0.85 for Type I cement and moist curing, respectively, in accordance with ACI 209R-92 (2008).

In addition, the predictions of the following equation from ACI 318-19 (2019) are also shown in Figure 8 for comparison:

$$E_{\mathrm{c}} = 4700\sqrt{f_c'} \tag{5}$$

It should be noted that in ACI 318-19 (2019), Eq. 5 is specified only for the 28-day modulus of elasticity (E_{c}), and f_c' in the equation is the 28-day compressive strength. However, for comparison purposes, Eq. 5 was used in the present study to predict the modulus of elasticity at various ages, making use of the corresponding compressive strength at the same age.

It is evident from Figure 8 that the equations from all three standards overestimate the test results of the present study for all the ages. The predictions of the ACI 318-19 equation (Eq. 5) appear to be closer to the test results than the other two equations (Eqs. 1 and 3). It is also interesting to note that compared with the data points of Group 1 with tap water, the data points of other groups with saltwater seem to be farther away from the three predicted curves. Furthermore, the discrepancy between the test result and the predicted curves seems to increase with the salinity of mixing water. The above observation suggests that for the same compressive strength, the modulus of elasticity of concrete may decrease with the salinity of mixing water. As a result, the three equations for the modulus of elasticity (e.g. Eqs. 1, 3, and 5) for freshwater concrete may not be applicable to saltwater concrete.

[Insert Figure 8]

5. CONCLUSIONS

This paper has presented a systematic experimental study on the effects of salinity of mixing water on the short-term properties of concrete. Saltwater with varying salinities from 0% to 250% of the world-average ocean salinity level was used in the concrete mixes. The following conclusions can be drawn based on the test results and discussions:

1. Isothermal calorimetry tests showed that the rate of hydration heat at early ages and the cumulative release of hydration heat both increase with the salinity of mixing water.

2. The rate of shrinkage increased with the salinity of mixing water, especially within the initial 21 days after casting. At the age of 90 days, the shrinkage strain of the concrete made with saltwater, with a salinity of 66 g/L, was over twice that of the concrete mixed with tap water.

3. The salinity of mixing water generally had a slight negative effect on the concrete strength after 14 days, while the concrete made with saltwater, with a salinity of up to 33 g/L, had a higher 1-day strength than that made with tap water. For the three groups of concrete made with saltwater having a salinity equal to or larger than 49.5 g/L, their strengths at various ages of up to 90 days were generally similar, and were all lower than the corresponding strengths of the concrete made with tap water.

4. The effect of mixing water salinity on the modulus of elasticity of concrete is generally similar to that on the concrete strength. For concretes with the same compressive strength, the modulus of elasticity may decrease as a result of the salinity of the mixing water.

ACKNOWLEDGEMENTS

The authors gratefully acknowledge the financial support provided by the Hong Kong Research Grants Council (Project No: T22-502/18-R) and The Hong Kong Polytechnic University (Project Account Code: 1-BBAG). The authors are also grateful to Prof. Alex Remennikov and A/Prof. Neaz Sheikh for supporting the first author to undertake a Research Student Attachment Program funded by and at The Hong Kong Polytechnic University.

REFERENCES

ACI. (2008). *Prediction of creep, shrinkage, and temperature effects in concrete structures* (Reapproved 2008). ACI 209R-92, Farmington Hills, Mich.

ACI. (2019). *Building code requirements for structural concrete and commentary.* ACI-318, Farmington Hills, Mich.

ASTM. (2014). *Standard test method for static modulus of elasticity and Poisson's ratio of concrete in compression*. ASTM C469/C469M-14, West Conshohocken, PA.

ASTM. (2015). *Standard test method for slump of hydraulic-cement concrete*. ASTM C143/C143M-15a, West Conshohocken, PA.

ASTM. (2017a). *Standard practice for measuring hydration kinetics of hydraulic cementitious mixtures using isothermal calorimetry*. ASTM C1679-17, West Conshohocken, PA.

ASTM. (2017b). *Standard test method for length change of hardened hydraulic-cement mortar and concrete*. ASTM C157-17, West Conshohocken, PA.

Bakhshi, M., Mobasher, B., & Soranakom, C. (2012). Moisture loss characteristics of cement-based materials under early-age drying and shrinkage conditions. *Construction and Building Materials*, 30, 413–425.

BS EN. (2000). *Cement. Composition, specifications and conformity criteria for common cements*. BS EN 197-1, British Standard Institution, London.

CEB-FIP. (2010). *Model code for concrete structures*. Thomas Telford Services Ltd., London.

Cheung, J., Jeknavorian, A., Roberts, L., & Silva, D. (2011). Impact of admixtures on the hydration kinetics of Portland cement. *Cement and Concrete Research*, 41(12), 1289–1309.

De Weerdt, K., Justnes, H., & Geiker, M. R. (2014). Changes in the phase assemblage of concrete exposed to sea water. *Cement and Concrete Composites*, 47, 53–63.

Dhondy, T., Remennikov, A., & Shiekh, N. M. (2019). Benefits of using sea sand and seawater in concrete: a comprehensive review, *Australian Journal of Structural Engineering*, 20(4), 280–289.

Gagg, C. R. (2014). Cement and concrete as an engineering material: An historic appraisal and case study analysis. *Engineering Failure Analysis*, 40, 114–140.

Gieskes, J. M., Elwany, H., Rasmussen, L., Han, S., Rathburn, A., & Deheyn, D. D. (2013). Salinity variations in the Venice Lagoon, Italy: results from the SIOSED project, May 2005-February 2007. *Marine Chemistry*, 154, 77–86.

Ghorab, H. Y., Hilal, M. S., & Kishar, E. A. (1989). Effect of mixing and curing waters on the behaviour of cement pastes and concrete part 1: microstructure of cement pastes. *Cement and Concrete Research*, 19(6), 868–878.

Ghorab, H. Y., Hilal, M. S., & Antar, A. (1990). Effect of mixing and curing waters on the behaviour of cement pastes and concrete Part 2: Properties of cement paste and concrete. *Cement and Concrete Research*, 20(1), 69–72.

Hansen, W. (1987). Drying shrinkage mechanisms in Portland cement pastes. *Journal of the American Ceramic Society*, 70(5), 323–328.

Hay, W. W., Wold, C. N., Söding, E., & Floegel, S. (2001). Evolution of sediment fluxes and ocean salinity. In: *Geologic Modeling and Simulation. Computer Applications in the Earth Sciences*. Springer, Boston, MA.

Hua, C., Acker, P., & Ehrlacher, A. (1995). Analyses and models of the autogenous shrinkage of hardening cement paste: I. Modelling at macroscopic scale. *Cement and Concrete Research*, *25*(7), 1457–1468.

Huang, B. T., Yu, J., Wu, J. Q., Dai, J. G., & Leung, C. K. Y. (2020). Seawater sea-sand engineered cementitious composites (SS-ECC) for marine and coastal applications, *Composites Communications*, 20, 100353.

Juenger, M. C. G., Monteiro, P. J. M., Gartner, E. M., & Denbeaux, G. P. (2005). A soft X-ray microscope investigation into the effects of calcium chloride on tricalcium silicate hydration. *Cement and Concrete Research*, 35(1), 19–25.

Kaushik, S. K. & Islam, S. (1995). Suitability of seawater for mixing structural concrete exposed to a marine environment. *Cement and Concrete Composites*, 17(3), 177–185.

Khatibmasjedi, M., Ramanthan, S., Suraneni, P., & Nanni, A. (2019). Shrinkage behavior of cementitious mortars mixed with seawater. *Advances in Civil Engineering Materials*, 8(2), 64-78.

Li, H., Farzadnia, N., & Shi, C. (2018). The role of seawater in interaction of slag and silica fume with cement in low water-to-binder ratio pastes at the early age of hydration. *Construction and Building Materials*, 185, 508–518.

Li, P., Li, W., Yu, T., Qu, F., & Tam, V. W. Y. (2020). Investigation on early-age hydration, mechanical properties and microstructure of seawater sea sand cement mortar. *Construction and Building Materials*, 249, 118776.

Li, Y., & Li, J. (2014). Capillary tension theory for prediction of early autogenous shrinkage of self-consolidating concrete. *Construction and Building Materials*, 53, 511–516.

Lu, J. X., Zhan, B. J., Duan, Z. H., & Poon, C. S. (2017). Improving the performance of architectural mortar containing 100% recycled glass aggregates by using SCMs. *Construction and Building Materials*, 153, 975–985.

Lura, P., Jensen, O. M., & Van Breugel, K. (2003). Autogenous shrinkage in high-performance cement paste: An evaluation of basic mechanisms. *Cement and Concrete Research*, 33(2), 223–232.

Makhlouf, A. S. H. (Ed.). (2014). *Handbook of smart coatings for materials protection*. Elsevier, Amsterdam.

NASA. (2014). Saltiest pond on earth. *https://earthobservatory.nasa.gov/images/84955/saltiest-pond-on-earth#:~:text=With%20a%20salinity%20level%20over,average%20salinity%20of%203.5%20percent.* (Accessed on 14 July 2020).

Nishida, T., Otsuki, N., Ohara, H., Garba-Say, Z. M., & Nagata, T. (2013). Some considerations for applicability of seawater as mixing water in concrete. *Journal of Materials in Civil Engineering*, ASCE, 27(7), B4014004.

NOAA. (2018). https://oceanservice.noaa.gov/facts/whysalty.html (accessed 21 June 2020).

Park, S. S., Kwon, S. J., & Song, H. W. (2011). Analysis technique for restrained shrinkage of concrete containing chlorides. *Materials and Structures*, 44, 475–486.

Pauw, A. (1960). Static modulus of elasticity of concrete as affected by density, *ACI Journal proceedings*, 57(12): 679–687.

Peterson, V.K., & Juenger, M. (2006). Hydration of tricalcium silicate: effects of $CaCl_2$ and sucrose on reaction kinetics and product formation, *Chemistry of Materials*, 18, 5798–5804.

Red Sea. (2017). Red sea salts, *Red Sea Product Catalog #R99344 _ENG_V17b*, 3–5.

Shayan, A. (2010). Effects of sea water on AAR expansion of concrete. *Cement and Concrete Research*, 40(4), 563–568.

Shi, Z. G., Shui, Z. H., Li, Q., and Geng, H. N. (2015). Combined effect of metakaolin and sea water on performance and microstructures of concrete. *Construction and Building Materials*, 74, 57–64.

Singh, N. B., & Ojha, P. N. (1981). Effect of $CaCl_2$ on the hydration of tricalcium silicate, *Journal of Material Science*, 16, 2675–2681.

Suryavanshi, A. K., Scantlebury, J. D., & Lyon, S. B. (1995). Pore size distribution of OPC & SRPC mortars in presence of chlorides. *Cement and Concrete Research*, 25(5), 980–988.

Suryavanshi, A. K., & Swamy, R. N. (1996). Stability of Friedel's salt in carbonated concrete structural elements. *Cement and Concrete Research*, 26(5), 729–741.

Taylor, M. A., & Kuwairi, A. (1978). Effects of ocean salts on the compressive strength of concrete. *Cement and Concrete Research*, 8(4), 491–500.

Teng, J. G., Yu, T., Dai, J. G., & Chen, G. M. (2011). FRP composites in new construction: current status and opportunities, in: *Proceedings of the 7th National Conference on FRP Composites in Infrastructure* [supplementary issue of *Industrial Construction,* 41(464), 58], Hangzhou, China, 15-16 October (Abstract, in Chinese).

Teng, J. G. (2014). Performance enhancement of structures through the use of fibre-reinforced polymer (FRP) composites, in: *Proceedings of the 23rd Australasian Conference on the Mechanics of Structures and Materials (ACMSM23)*, Baron Bay, New South Wales, Australia, 9-12 December (Abstract).

Teng, J. G., Xiang, Y., Yu, T., & Fang, Z. (2019). Development and mechanical behaviour of ultra-high-performance seawater sea-sand concrete. *Advances in Structural Engineering*, 22(14), 3100-3120.

Uddin, T., Hidenori, H., & Yamaji, T. (2004). Performance of seawater-mixed concrete in the tidal environment. *Cement and Concrete Research*, 34(4), 593–601.

Vanhanen, J., Hyvärinen, A. P., Anttila, T., Raatikainen, T., Viisanen, Y., & Lihavainen, H. (2008). Ternary solution of sodium chloride, succinic acid and water; surface tension and its influence on cloud droplet activation. *Atmospheric Chemistry and Physics*, 8(16), 4595–4604.

Xiao, J., Qiang, C., Nanni, A., & Zhang, K. (2017). Use of sea-sand and seawater in concrete construction: current status and future opportunities. *Construction and Building Materials*, 155, 1101–1111.

Younis, A., Ebead, U., Suraneni, P., & Nanni, A. (2018). Fresh and hardened properties of seawater-mixed concrete. *Construction and Building Materials*, 190, 276–286.

Younis, A., Ebead, U., Suraneni, P., & Nanni, A. (2019). Microstructure investigation of seawater vs. freshwater cement pastes. In: *Proceedings, 10th International Structural Engineering and Construction Conference: Interdependence between Structural Engineering and Construction Management (ISEC 2019)*, Chicago, Illinois, United States, 20–25 May.

LIST OF FIGURES

LIST OF TABLES

Tables

Table 1. Mix Proportions

Concrete Mix	OPC (kg/m^3)	RS (kg/m^3)	CG (kg/m^3)	Salt dose (g/L)	Water (kg/m^3)
Group 1	350	700	1100	0	224
Group 2	350	700	1100	18	224
Group 3	350	700	1100	36	224
Group 4	350	700	1100	54	224
Group 5	350	700	1100	72	224
Group 6	350	700	1100	90	224

Note: OPC - ordinary Portland cement; RS - river sand; CG - crushed granite.

Table 2. Chemical and phase compositions of cement

Chemical composition	% by weight
SiO_2	21.60
Fe_2O_3	0.41
Al_2O_3	5.16
CaO	65.55
TiO_2	0.17
SO_3	3.63
MgO	2.40
Na_2O	--
K_2O	0.26
ZnO	--
ZrO_2	--
Phase composition	**% by weight**
C_3S	57.00
C_2S	19.02
C_3A	12.99
C_4AF	1.24

Table 3. Chemical compositions of natural seawater, saltwater and tap water (in g/L)

Ion	Seawater average (Dickson and Goyet 1994)	Tap water for Group 1	Natural seawater		Saltwater for Group 3
			Chek Lap Kok, Hong Kong	Repulse Bay, Hong Kong	
F^-	0.0013	0.0005	0.0000	0.0000	0.0000
Cl^-	19.3524	0.0116	18.1526	18.3124	17.7812
Br^-	0.0673	0.0000	0.0659	0.0738	0.0617
SO_4^{2-}	2.7123	0.0176	1.6750	1.6998	1.7438
NO_2^-	--	0.0000	0.0000	0.0649	0.0000
NO_3^-	--	0.0099	0.0000	0.0314	0.0285
PO_4^{3-}	--	0.0000	0.0000	0.0000	0.0000
Li^+	--	0.0000	0.0007	0.0006	0.0006
Na^+	10.7837	0.0091	10.4194	11.1388	11.0738
NH_4^+	--	0.0000	0.0000	0.0179	0.0057
K^+	0.3991	0.0035	0.3544	0.3926	0.4329
Mg^{2+}	1.2837	0.0018	1.2152	1.3410	1.2913
Ca^{2+}	0.4121	0.0169	0.3582	0.4535	0.4609
Salinity	35.0119	0.0709	32.2413	33.5268	32.8803

Table 4. Summary of key results

Group	Slump (mm)	$f'_{c,1d}$ (MPa)	$f'_{c,7d}$ (MPa)	$E_{c,\ 7d}$ (GPa)	$f'_{c,14d}$ (MPa)	$E_{c,\ 14d}$ (GPa)	$f'_{c,28d}$ (MPa)	$E_{c,\ 28d}$ (GPa)	$f'_{c,60d}$ (MPa)	$E_{c,\ 60d}$ (GPa)	$f'_{c,90d}$ (MPa)	$E_{c,\ 90d}$ (GPa)
Group 1	50	16.9	31.0	26.9	33.7	27.6	35.7	24.4	36.5	26.0	35.8	26.3
Group 2	60	18.4	31.3	24.3	30.8	25.7	32.9	24.0	32.8	24.0	32.7	23.9
Group 3	60	20.2	30.1	24.8	32.4	24.3	32.2	22.5	33.6	24.1	33.2	23.3
Group 4	80	18.1	28.4	21.4	27.3	22.1	29.5	20.9	30.8	20.6	30.7	21.0
Group 5	90	16.4	26.5	22.2	28.3	21.9	27.2	20.9	29.5	20.7	29.7	20.4
Group 6	40	17.2	26.3	19.7	29.2	21.9	29.8	21.4	30.7	20.5	30.5	20.2

Figures

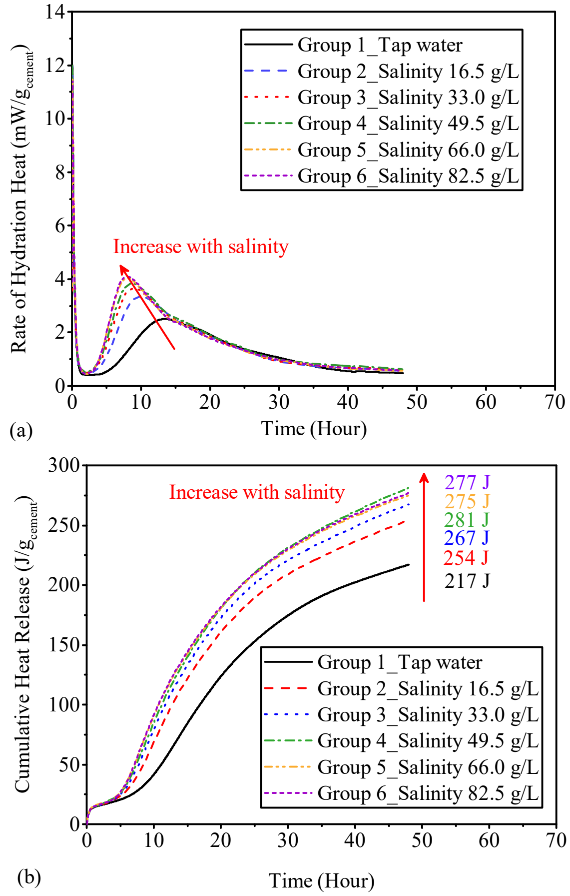

Figure 1. Heat evolution of cementitious pastes with various salinities: (a) rate of hydration heat per gram of cement; and (b) cumulative heat release per gram of cement.

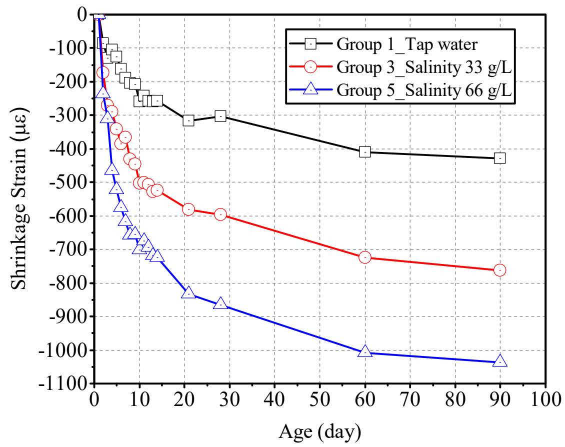

Figure 2. Time histories of shrinkage of Groups 1, 3 and 5.

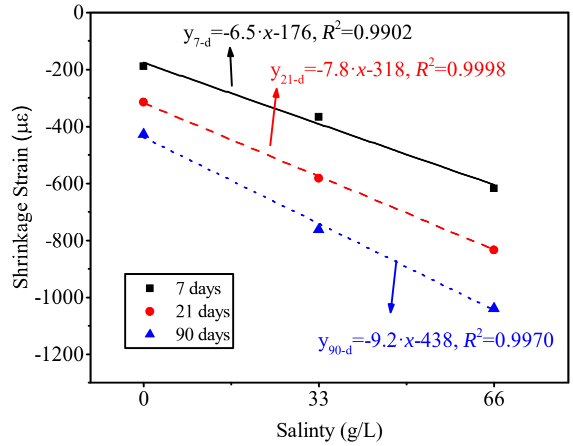

Figure 3. Relationship between shrinkage and water salinity.

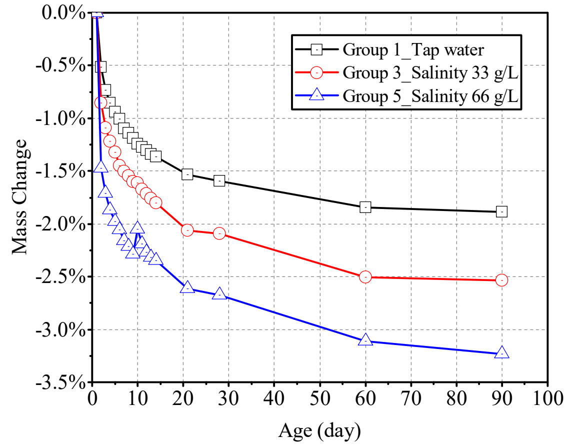

Figure 4. Time histories of mass change of Groups 1, 3 and 5.

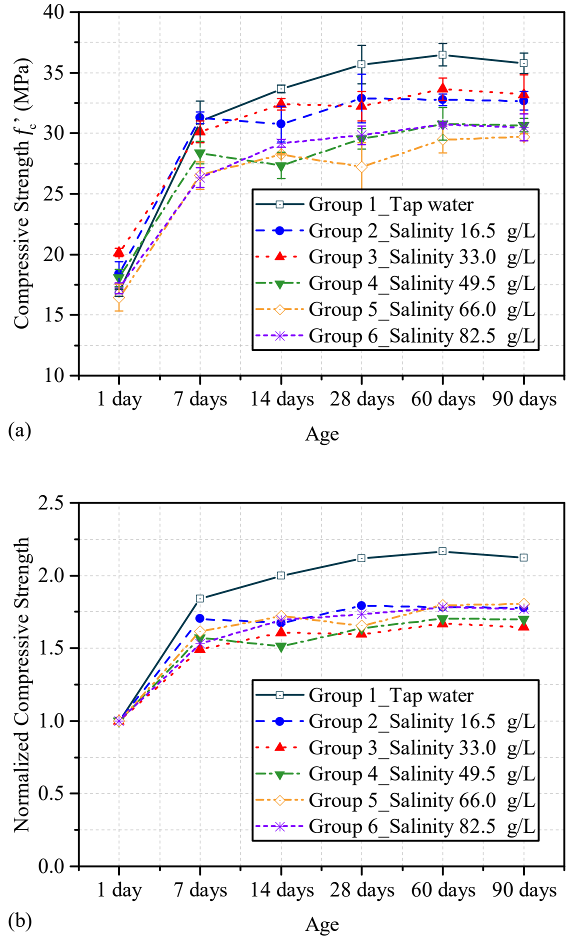

Figure 5. Strength development of concrete: (a) compressive strength; and (b) normalized compressive strength.

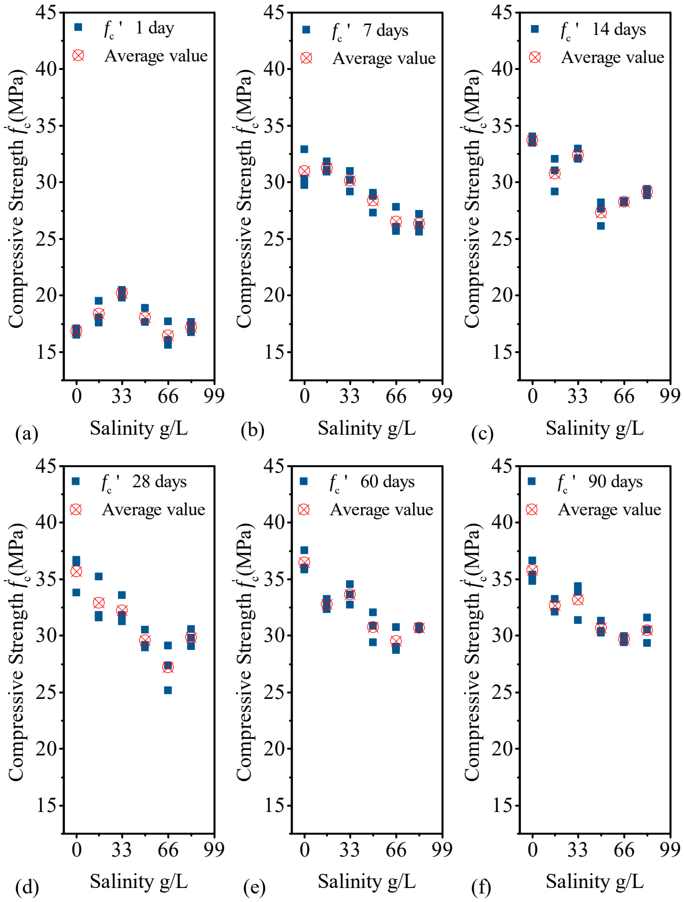

Figure 6. Compressive strengths at: (a) 1 day; (b) 7 days; (c) 14 days; (d) 28 days; (e) 60 days and (f) 90 days.

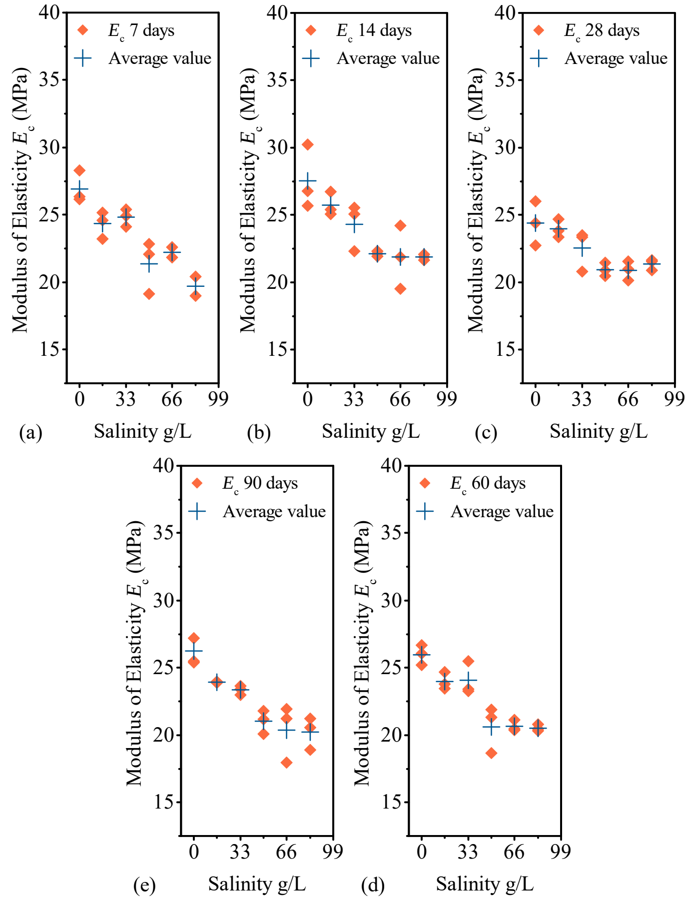

Figure 7. Values of modulus of elasticity at: (a) 7 days; (b) 14 days; (c) 28 days; (d) 60 days and (e) 90 days.

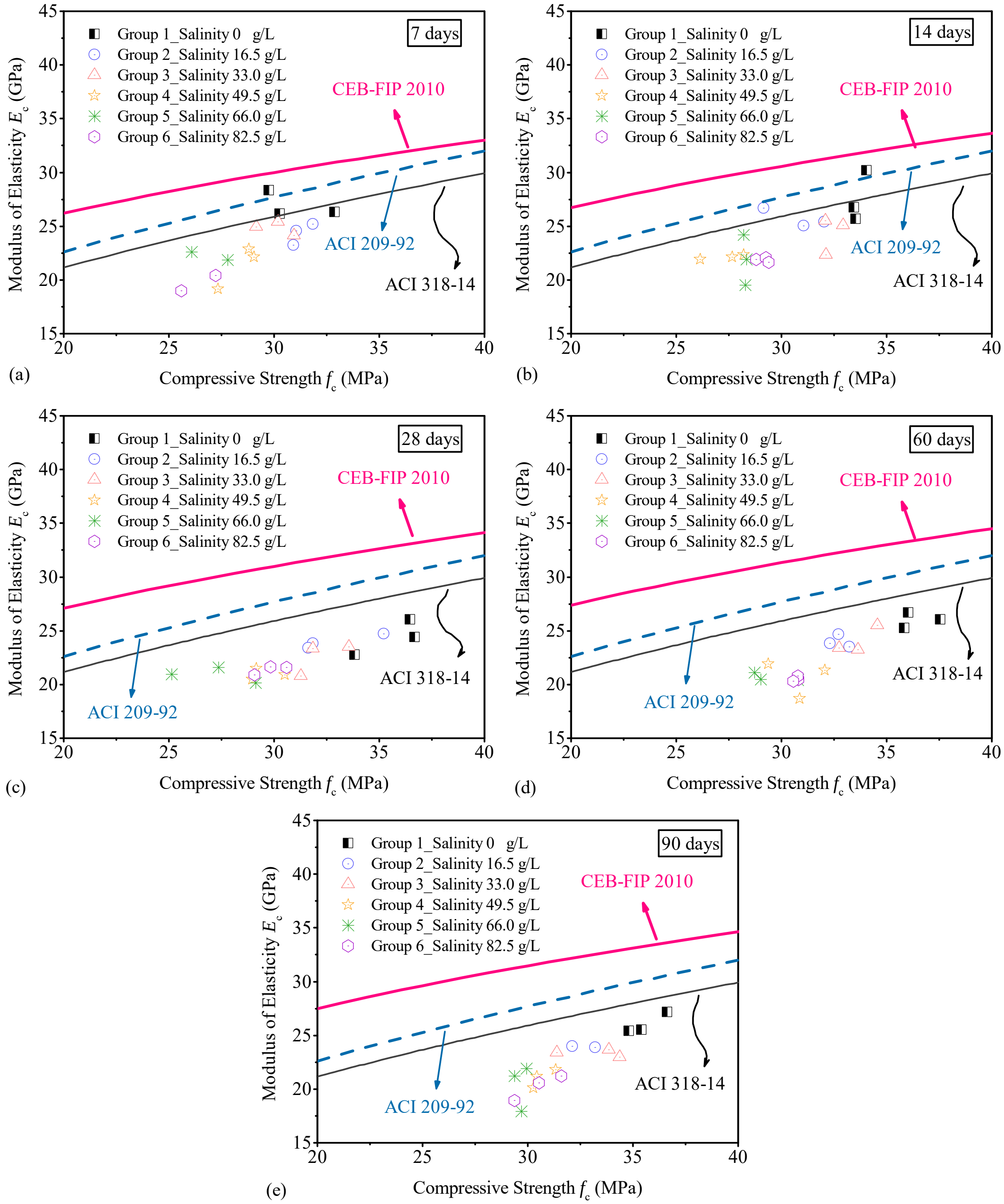

Figure 8. Modulus of elasticity versus compressive strength at: (a) 7 days; (b) 14 days; (c) 28 days; (d) 60 days; and (f) 90 days.